

## A Case Study of Excessive Rainfall Centered Around Wellsville, New York, 20–21 June 1972

LANCE F. BOSART AND FREDERICK H. CARR

*Department of Atmospheric Science, State University of New York at Albany, Albany, N.Y. 12222*

(Manuscript received 25 July 1977, in final form 23 November 1977)

### ABSTRACT

The pre-tropical storm Agnes rainstorm across western New York and Pennsylvania is analyzed using conventional surface and aerological data. Hourly precipitation maps and surface maps showed the north-eastward motion and intensification of a developing rain area over eastern Kentucky at 1200 GMT 20 June 1972. This area remained a separate entity from the main Agnes rainshield. Nonlinear balanced omega as well as kinematic omega computations suggest that a weak short wave in the mid and upper troposphere provided the initial triggering mechanism for the growth of the rain area. Plentiful moisture was available from the Agnes circulation to the south and the western Atlantic. Latent heat release then played a dominating role in modifying the resulting vertical velocity patterns. Finally, some possible general forecast considerations are suggested by these results.

### 1. Introduction

Hurricane Agnes of June 1972 proved to be one of the most destructive storms ever to strike the continental United States with most of the damage coming from excessive rainfall. An overview of the meteorological and climatological factors associated with this destructive storm can be found in a report by DeAngelis and Hodge (1972). This paper will concentrate on trying to understand the meteorological factors responsible for the initial development of heavy rains across southwestern New York and northwestern Pennsylvania prior to the arrival of Agnes and prior to the extratropical phase of the storm. Analyses of surface rainfall, surface and upper level moisture convergence and vorticity, kinematic vertical velocities and nonlinear balanced vertical velocities will be presented as a part of the documentation. Details of the relevant dynamics involved in the conversion of tropical storm Agnes itself into an extratropical disturbance can be found in DiMego (1977).

Fig. 1 shows the location of the hourly recording raingage stations used in this investigation. The heaviest rains were concentrated around Wellsville, N.Y. (position shown on map). Table 1 gives the daily rainfall at Wellsville throughout the course of the storm. This rain fell in two distinct bursts as can be seen from Fig. 2 which shows the cumulative hourly precipitation at Wellsville. The first burst occurred on 20–21 June and accounted for 60% of the total storm rainfall. This was the pre-Agnes stage with the cyclone itself centered over South Carolina. Rainfall, which was very light during the day on the

21st, became quite heavy again late on the 22nd as Agnes moved northward and then took on extra-tropical characteristics as it looped westward across Pennsylvania.

Detailed hourly precipitation and surface analyses were constructed using radar data, WBAN 10 forms and NOAA hourly precipitation bulletins obtained from the National Climatic Center (NCC) in Asheville, N.C. Hourly precipitation data for Ontario were obtained from the Canadian Atmospheric Environment Service. Checked radisonde and rawinsonde data on magnetic tape were also obtained from the NCC. A goal was to concentrate on the important small-scale features which are often smoothed out or lost by objective analysis routines designed to retain synoptic-scale features in numerical forecast models.

### 2. Synoptic situation

The overall synoptic situation is shown in Fig. 3. Tropical storm Agnes drifted slowly northeastward across Georgia in the 12 h period ending 0000 GMT<sup>1</sup> 21 June while further to the west a frontal trough edged slowly eastward. A pronounced surface ridge oriented east-northeast–west-southwest runs from southern New England to eastern Kentucky.

Abundant moisture was available in the lower half of the troposphere throughout the Agnes circulation and in a narrow tongue extending northward along the Appalachians, as can be seen in the surface to

<sup>1</sup> Greenwich Mean Time is used throughout the paper; the symbol Z is used in the figures.

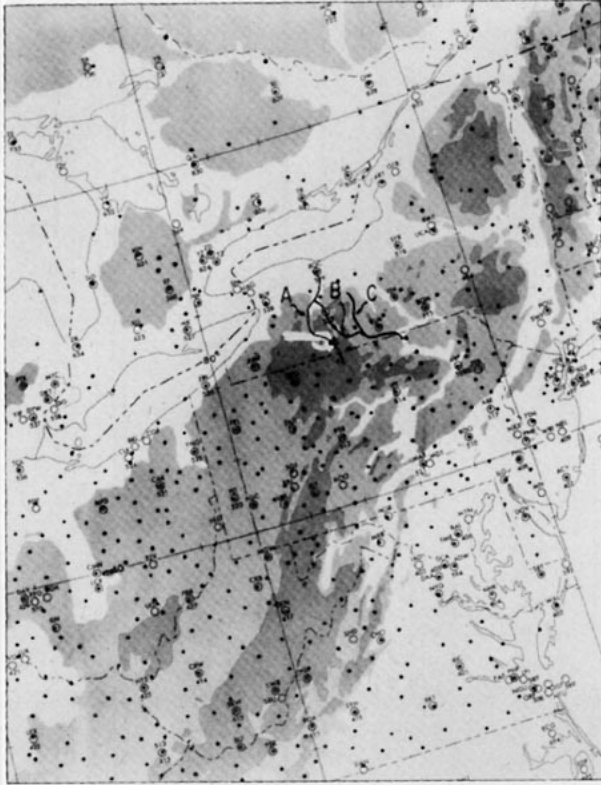


FIG. 1. Location of hourly recording raingage stations (black dots) and Wellsville, N.Y. (solid triangle). Flooding occurred along the three rivers indicated by A (Genessee), B (Canisteo) and C (Chemung).

500 mb mean relative humidity chart for 0000 GMT 21 June (Fig. 3d). The lifted index chart for the same time period (Fig. 3c) also indicates the potential for convection from the lower Ohio valley northeastwards to Ontario. Both of these charts were reconstructed from the original National Meteorological Center (NMC) analyses after the receipt of some additional and corrected data not available in real time. Squall line activity was noted across southeastern Michigan, western Ohio and Ontario a few hours prior to 0000 GMT on 21 June in advance of the slow moving frontal trough. This activity dissipated as it moved eastward.

3. Surface rainfall analyses

Fig. 4a shows the cumulative 6 h precipitation for the period ending 1800 GMT 20 June. Two dis-

TABLE 1. Daily rainfall (cm) at Wellsville, N. Y. 20-23 June 1972.

20 June	3.1
21 June	19.3
22 June	9.9
23 June	1.5
Total	33.8

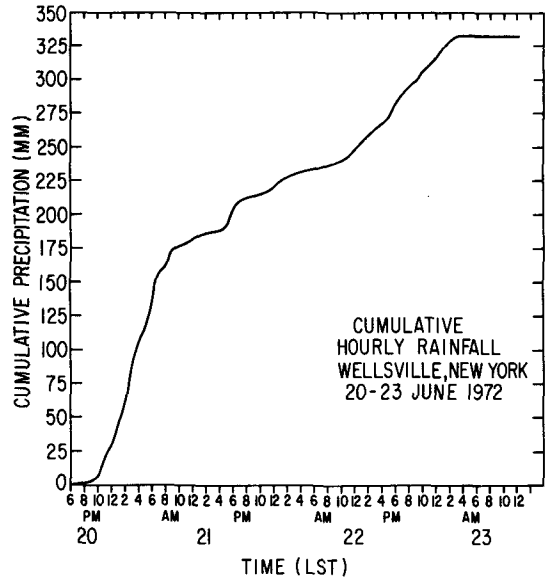


FIG. 2. Cumulative hourly rainfall (mm) at Wellsville, N.Y., 20-23 June 1972. Discrepancy between Table 1 and Fig. 2 is that additional rain fell later in the day on the 23rd.

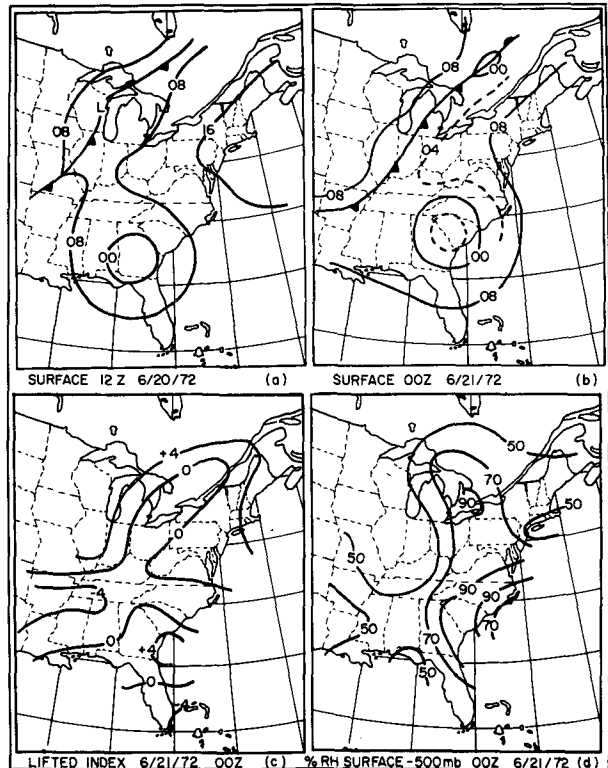


FIG. 3a. Surface pressure (mb) 1200 GMT 20 June 1972.

FIG. 3b. Surface pressure (mb) 0000 GMT 21 June 1972.

FIG. 3c. Lifted index 0000 GMT 21 June 1972.

FIG. 3d. Mean surface of 500 mb relative humidity (%) for 0000 GMT 21 June 1972.

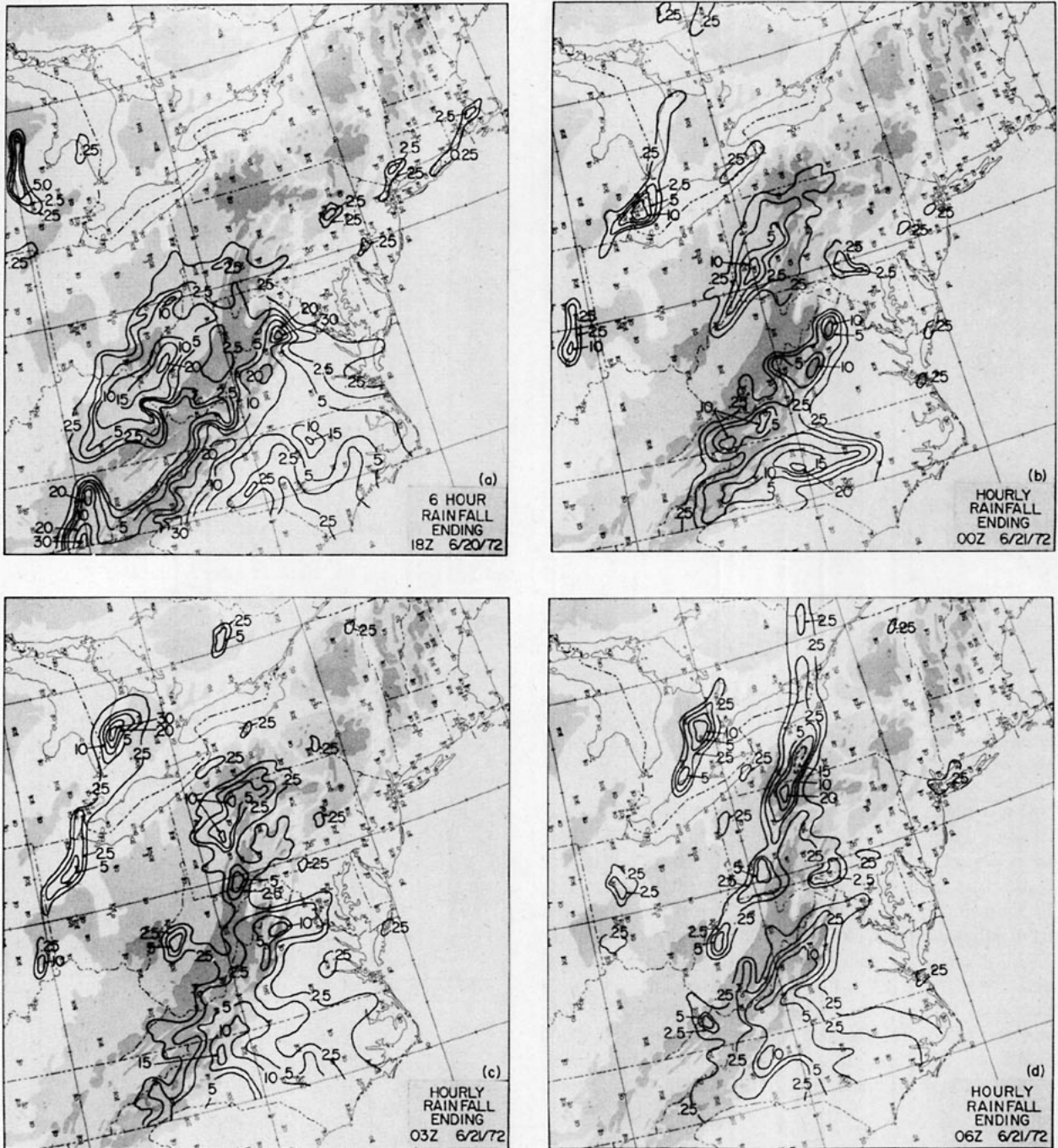


FIG. 4. Cumulative 6 h precipitation (mm) ending 1800 GMT 20 June 1972 (a) and hourly precipitation (mm) ending 0000 GMT 21 June (b), 0300 GMT 21 June (c), 0600 GMT 21 June (d), 0900 GMT 21 June (e), 1200 GMT 21 June (f) and 1800 GMT 21 June (g).

tinct rainfall areas are evident on either side of the Appalachians. The area to the south and east is associated with the primary Agnes circulation. Orographic enhancement of precipitation in western North Carolina and Virginia is clearly indicated. The detailed hourly precipitation maps and analyses established that the Ohio Valley rainfall area evolved northeastward from eastern Kentucky shortly before 1200 GMT

on the 20th. This area intensified northeastward in a narrow band along the Ohio river with maximum hourly rainfalls in the vicinity of 0.6 cm.

The belt of relative dryness across eastern West Virginia and extreme southwestern Virginia is well documented by raingage stations as can be seen from their distribution in Fig. 1. Six-hour rainfall totals were of the order of 1–2 mm with trace amounts to

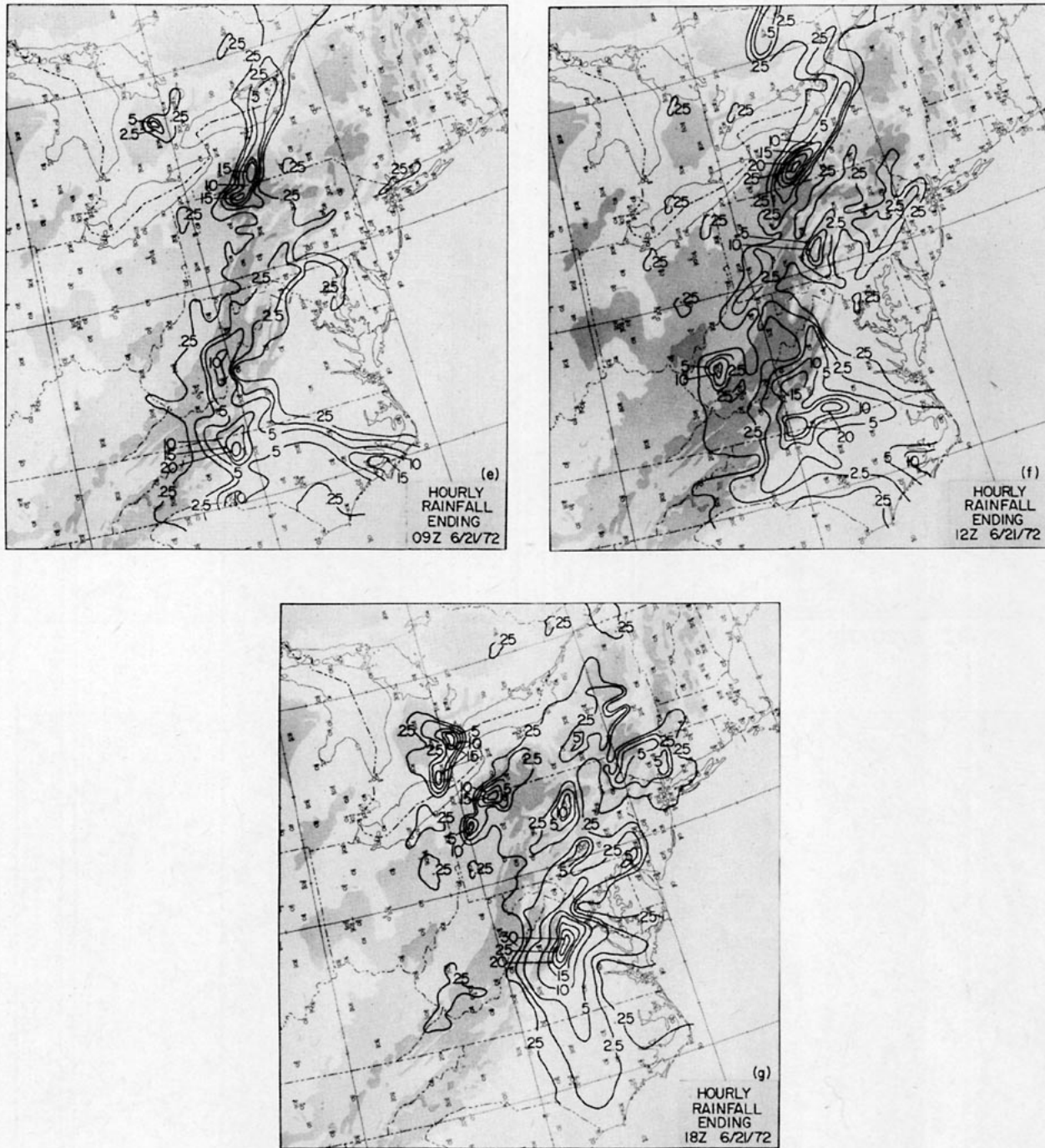


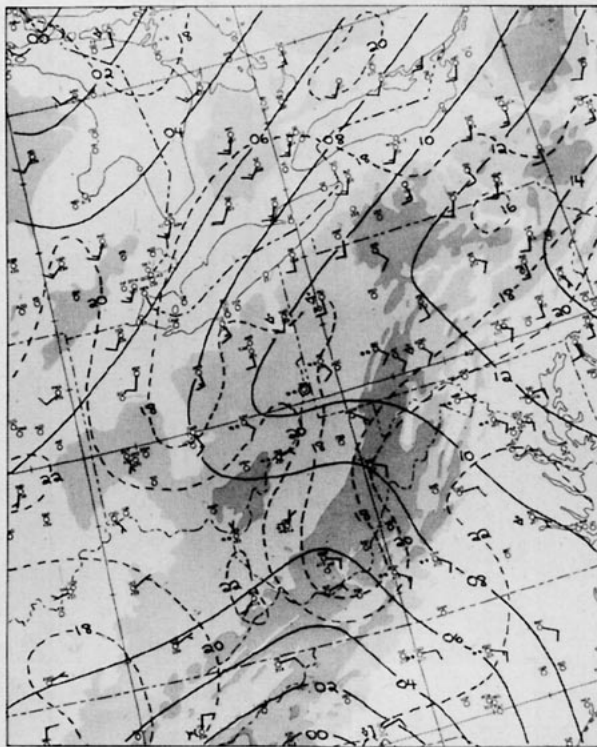
FIG. 4. (Continued)

the south. An orographic explanation for the dry area sandwiched between the two wet areas is not convincing in view of the topography of the region. The two rainfall regimes appear to be distinct phenomena.

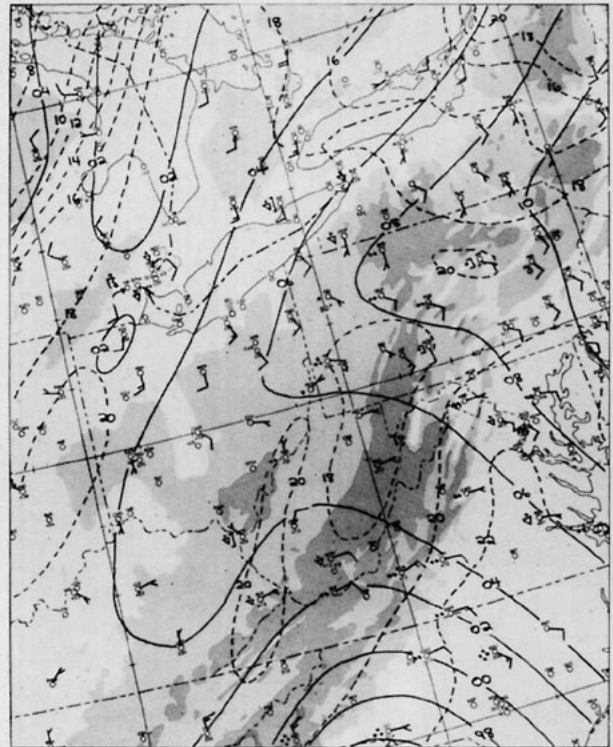
The next map (Fig. 4b) shows the precipitation field for the hour ending 0000 GMT 21 June. The Ohio Valley rain area has advected into western Pennsylvania (supported by hourly analyses not

shown) with a small area in excess of 1 cm. The narrowness of the zone in comparison to its length suggests the possibility of a squall line. However, this is not substantiated by the available surface and radar data. Buffalo WSR-57 radar information suggests uniform cells with only a few tops reaching just over 6 km. The RHI counterpart of the Pittsburgh WSR-57 was unfortunately inoperative during the

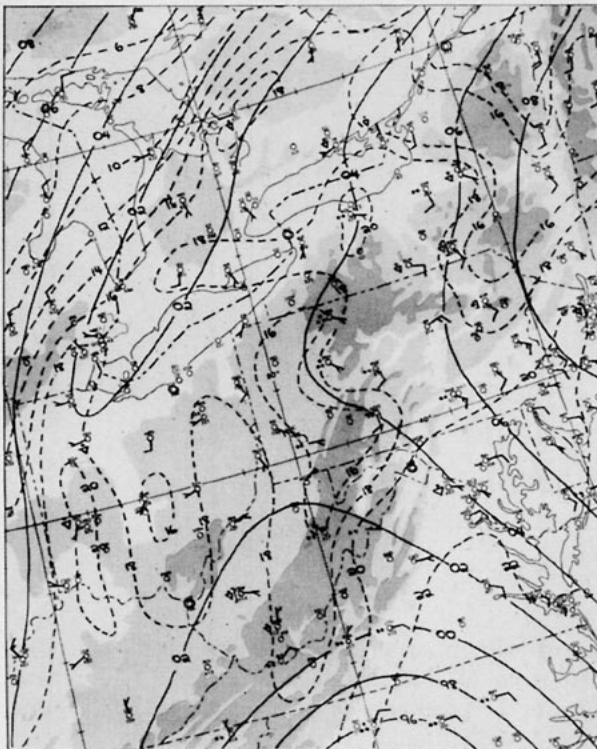




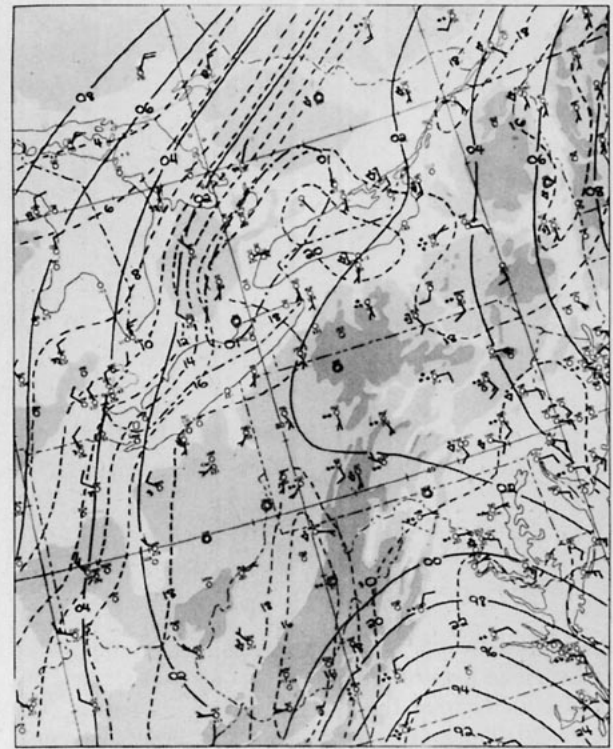
18Z 6/20/72 (a)



00Z 6/21/72 (b)



06Z 6/21/72 (c)



12Z 6/21/72 (d)

FIG. 5a. Surface sectional for 1800 GMT 20 June 1972: isobars (mb), solid lines every 2 mb; dew-point temperature ( $^{\circ}\text{C}$ ), dashed lines every  $2^{\circ}\text{C}$ ; winds in knots and significant present weather according to conventional practice.

FIG. 5b. As in Fig. 5a except for 0000 GMT 21 June 1972.

FIG. 5c. As in Fig. 5a except for 0600 GMT 21 June 1972.

FIG. 5d. As in Fig. 5a except for 1200 GMT 21 June 1972.

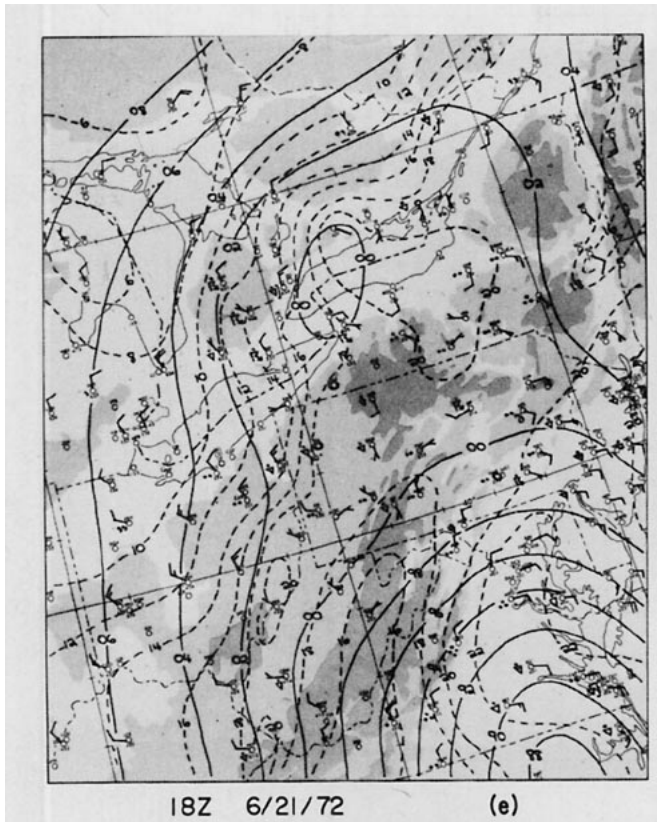


FIG. 5e. As in Fig. 5a except for 1800 GMT 21 June 1972.

storm period. Corresponding surface weather reports suggested a steady type of rainfall of moderate to heavy intensity.

Again, the Pennsylvania rain area is a distinct entity from the Agnes rainshield further to the south, as is the case in the preceding 6 h for which analyses are not shown. Note also (Fig. 4b) the area of precipitation extending from Canada across Lake Huron into extreme northwestern Ohio. This latter area is associated with a squall line that developed in advance of the Great Lakes trough. Maximum tops in this line were approaching 15 km according to Detroit WSR-57 radar.

During the next 3 h the Pennsylvania rain area continued to intensify slowly northeastward with a general area exceeding 0.5 cm evident in northwestern Pennsylvania by the hour ending 0300 GMT 21 June (Fig. 4c). Clearly, the origin of the flood potential was due to the persistence of moderate intensity rainfall (see Fig. 2).

By 0600 on the 21st (Fig. 4d) the area of maximum rainfall rate is centered over southwestern New York with isolated hourly totals reaching 2.5 cm (not shown on map). Buffalo radar reports a maximum top of 7.5 km centered over the area of heaviest rain. The radar data coupled with Canadian hourly precipitation reports support the northeastward extension of the rainshield across eastern Lake Ontario and on

into Canada. Again, the Agnes rainshield to the south remains a separate entity while the squall line activity to the west continues to dissipate.

Between 0600 and 0900 (Fig. 4e) the southwestern New York precipitation area was relatively stationary with individual cells showing little motion according to Buffalo radar. Isolated amounts approached 2.5 cm (not resolvable on figures). The Agnes rainshield to the south is still separate but the distinction is not as pronounced as previously.

Continued very slow northeastward movement of the New York rainstorm is evident by 1200 GMT (Fig. 4f). A gradual merger with the primary Agnes rainshield to the south is also noted. After 1200 the northern rain area weakened rapidly as the southern area became more dominant while expanding northward. This is evident from the 1800 map (Fig. 4g) along with the redevelopment of convective activity to the west ahead of the approaching surface frontal trough.

#### 4. Surface sectionals

Detailed surface sectionals are presented in Fig. 5 at 6 h intervals beginning 1800 GMT 20 June (Fig. 5a) and ending 1800 on the 21st (Fig. 5e). Surface winds and present weather are superimposed on a surface

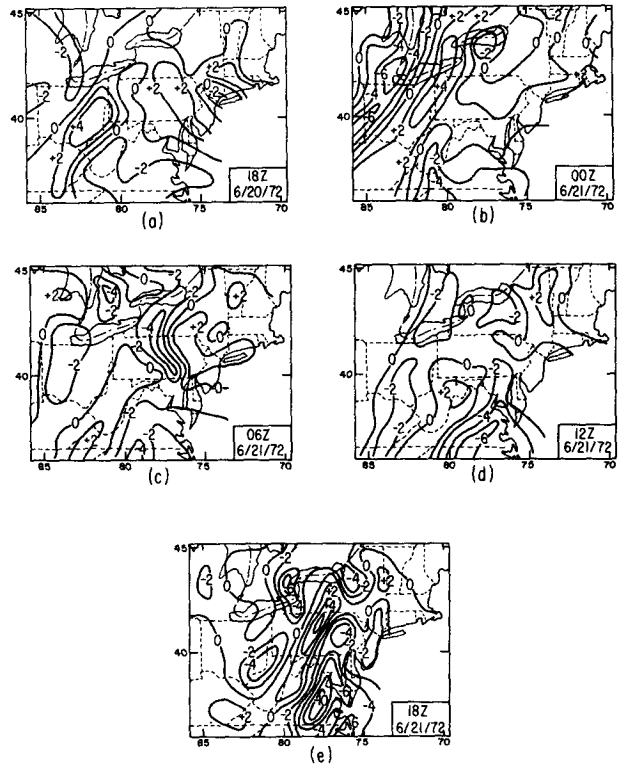


FIG. 6. Surface moisture flux convergence  $-\nabla \cdot qV$  ( $10^{-7} \text{ s}^{-1}$ ) for 1800 GMT 20 June 1972 (a), 0000 GMT 21 June 1972 (b), 0600 GMT 21 June 1972 (c), 1200 GMT 21 June 1972 (d), and 1800 GMT 21 June 1972 (e).

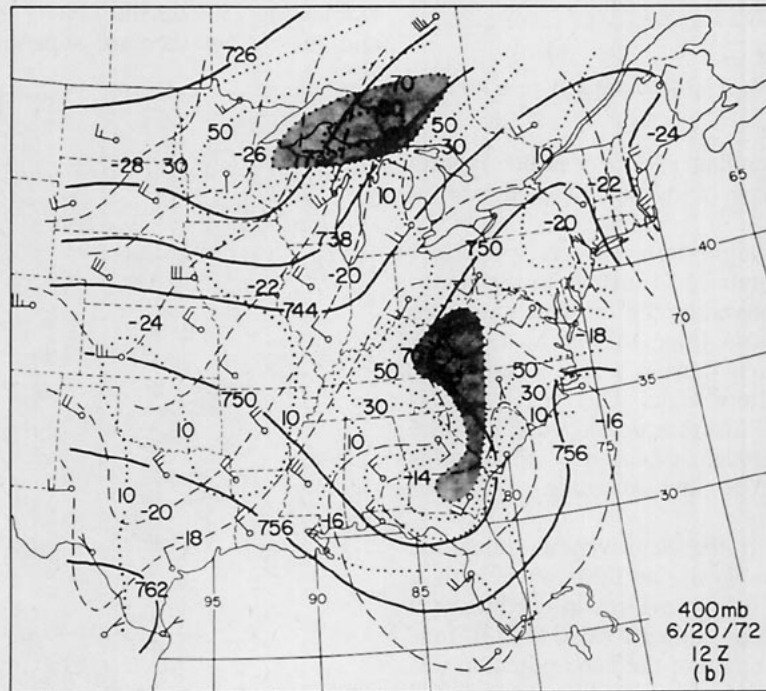
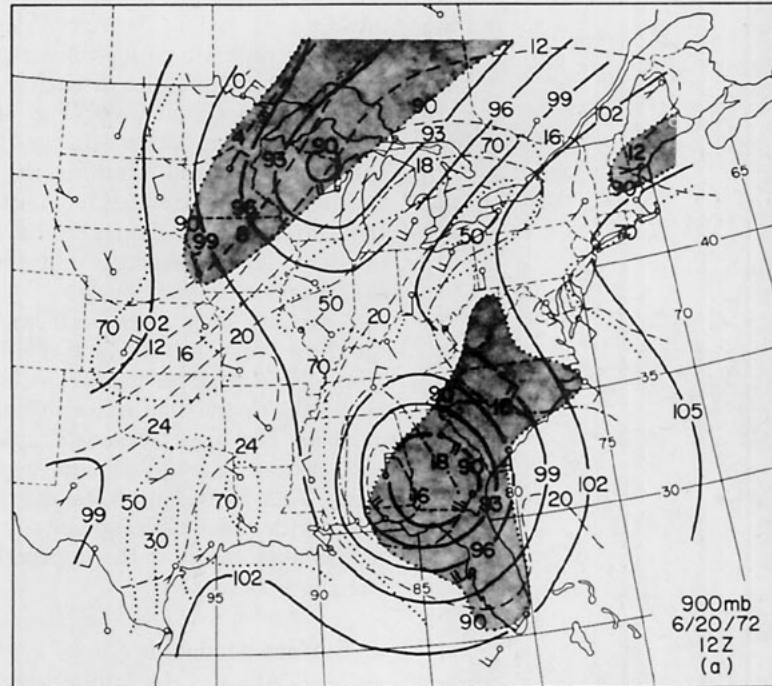


FIG. 7a. 900 mb height (dam), heavy solid lines; temperature ( $^{\circ}\text{C}$ ), thin dashed lines (intermediate  $18^{\circ}\text{C}$  isotherm dash-dotted line); and relative humidity (%), dotted lines with area of  $\text{RH} \geq 90\%$  stippled. Observed winds are plotted in  $\text{m s}^{-1}$  for 1200 GMT 20 June 1972.

FIG. 7b. As in Fig. 7a except for 400 mb 1200 GMT 20 June 1972 except the area of  $\text{RH} \geq 70\%$  is now stippled.

pressure and dew-point temperature analysis. The dominant feature of the 1800 GMT 20 June map (Fig. 5a) is the east-northeast-west-southwest oriented

pressure ridge across Pennsylvania and Ohio. The Ohio Valley rain area of Fig. 4a extends through this ridge line accompanied by a tongue of relatively high

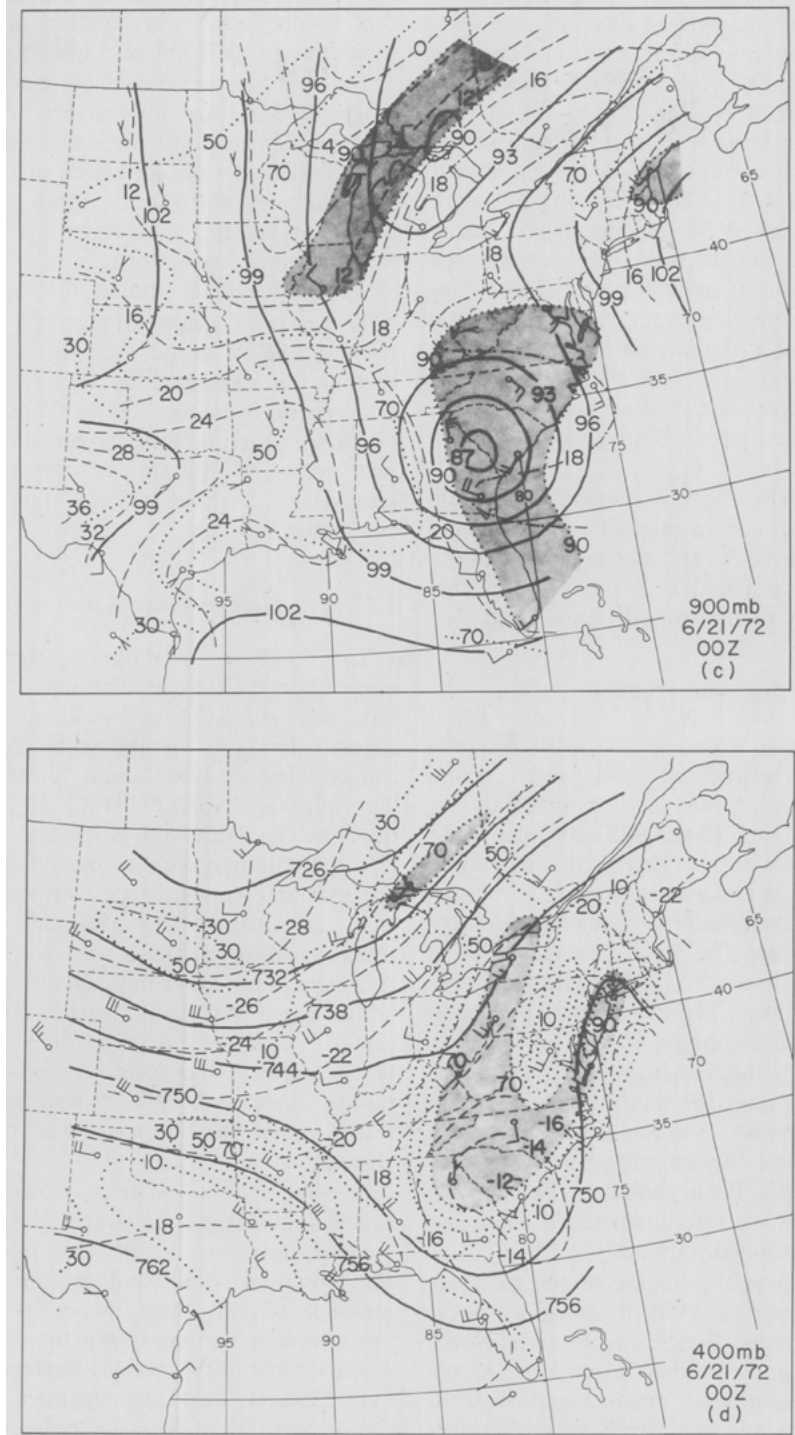


FIG. 7c. As in Fig. 7a except for 900 mb 0000 GMT 21 June 1972.  
 FIG. 7d. As in Fig. 7b except for 400 mb 0000 GMT 21 June 1972.

dew-point air. Another tongue of high dew-point air extends across Indiana into central Michigan in association with the developing convective activity in that region. Meanwhile the separate Agnes circulation and rainshield to the south is clearly evident.

Little change is evident in the ridge position and

orientation by 0000 (Fig. 5b). The western Pennsylvania rain area (Fig. 4b) is still centered along and just to the south of this ridge line. The Agnes rainshield is relatively stationary with upslope conditions prevailing in favorable regions of Virginia while the frontal trough continues to advance across Michigan.



A significantly different pattern emerges by 0600 (Fig. 5c) as a weak east-west oriented surface pressure trough is evident across western New York. The heavy rain in western New York (Fig. 4d) is now embedded in this weak surface pressure trough in the southwesterly surface geostrophic flow. No significant change is seen elsewhere. By 1200 (Fig. 5d) the weak east-west pressure trough is located over the extreme eastern end of Lake Ontario, somewhat downstream of the region of heaviest precipitation. A separate cyclonic circulation is just becoming evident a little north of the eastern end of Lake Erie although rainfall amounts are very light and scattered. Agnes continues to edge north-northeastward although the east-west oriented ridge line across Pennsylvania remains visible.

In the following 6 h (Fig. 5e) the developing cyclonic circulation center continued to intensify over extreme western Lake Ontario while the downstream trough dissipated. Renewed convective activity with this system is also evident in the rainfall maps (Fig. 4g).

### 5. Surface moisture flux convergence

Surface moisture flux convergence  $-\nabla \cdot qV_h$  was computed on a  $0.5^\circ$  latitude-longitude mesh across the northeastern United States at 3 h intervals for the 24 h period beginning 1800 GMT 20 June. Subjective analyses of temperature, dew-point depression, pressure, isogons and isotachs were prepared from all available first- and second-order civilian and military surface observations, and the results tabulated on a  $0.5^\circ$  mesh. A simple centered finite difference was used in the computations. The results are presented in Fig. 6 at 6 h intervals beginning at 1800 on the 20th.

Fig. 6a shows two distinct moisture flux convergence regions separated by a moisture flux divergence region across central Ohio. The eastern flux convergence region is associated with Agnes with a weak tongue extending into western Pennsylvania. The western flux convergence region is a forerunner to the Michigan convective regime mentioned previously.

By 0000 (Fig. 6b) a strengthening of the moisture flux convergence pattern is evident along a south-eastern Michigan-Indiana line, and western North Carolina. Little change is evident elsewhere. Agreement with the observed rainfall maxima near Detroit, central North Carolina and the Carolina and Virginia mountains is rather good. The western Pennsylvania rainfall maximum is not, however, well defined by the surface moisture flux convergence pattern.

The situation changes somewhat by 0600 (Fig. 6c). Now a narrow, well-defined tongue of moisture flux convergence is seen across western Pennsylvania and New York, in good agreement with the central and northern end of the observed rainfall area. A consideration of Figs. 6b and 6c suggests that it is likely

that the maximum over Indiana moves northeastward to southeastern Michigan while intensifying.

The pattern is somewhat more chaotic by 1200 (Fig. 6d). Moisture flux convergence is still seen across western Pennsylvania with a weak center in central New York and a stronger area east of the Appalachian mountains associated with Agnes to the south. A separate moisture flux convergence center is seen across extreme southern Ontario in the vicinity of a newly developing cyclonic circulation center (Fig. 6d).

The pattern again strengthens by 1800 (Fig. 6e) with an area of pronounced flux convergence centered east of the Virginia Blue Ridge mountains extending northwards into east-central Pennsylvania. Likewise, a strong moisture flux convergence center is evident just west of Buffalo as the cyclonic circulation strengthens in that area accompanied by renewed convective activity.

### 6. Upper air parameters and computations

The upper air data used in this investigation were also obtained from the National Climatic Center. The data were available every 50 mb in addition to significant levels of temperature, moisture and wind. Subjectively analyzed maps for 900 and 400 mb are shown in Fig. 7 for 1200 GMT 20 June and 0000 GMT 21 June. In both 900 mb maps Agnes is seen as a closed circulation regime embedded in an area of weak thermal gradient with the warmest air located to the east and north of the immediate center. An area of weak warm advection is seen northeast of the center. A much more baroclinic circulation regime is noted across the Great Lakes with warm advection across eastern Michigan into Ontario along and just ahead of the surface cold front. A region with relative humidity in excess of 90% is also seen extending northward along the Appalachians east of the Agnes circulation.

At 400 mb no separate closed circulation center exists above Agnes. A warm core circulation is still evident, however, at both time periods. Further north the observed wind and height fields suggest the presence of two short waves by 0000. The eastern short wave is moving into a tongue of 70% or greater relative humidity across western New York and Pennsylvania. This zone expanded northeastward from the previous 12 h. A separate dry center is seen across central Pennsylvania with another very moist region to the east along the coast.

Subjective analyses of temperature, relative humidity, isogons and isotachs were prepared for the 900-200 mb levels at 100 mb intervals for 1200 GMT 20 June and 0000 GMT 21 June 1972. The analyses were then tabulated on a  $1^\circ$  latitude-longitude mesh covering the eastern and central United States and southern Canada. Relative vorticity and moisture

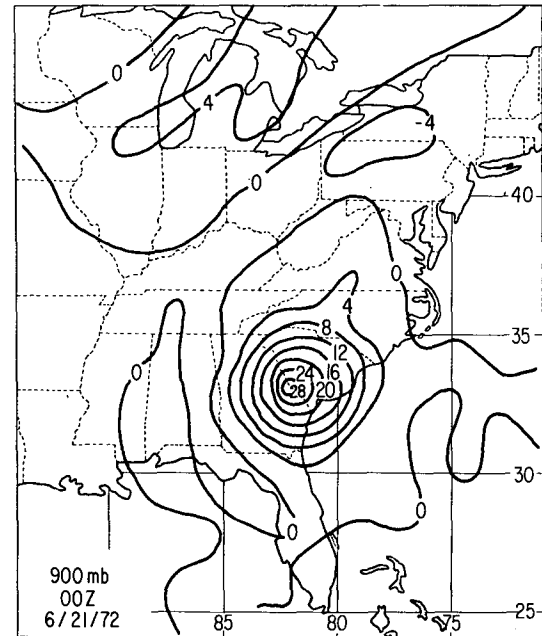
convergence were then computed from the tabulated data using a simple centered finite difference scheme.

The relative vorticity structure at 900 and 400 mb is shown in Fig. 8 for 0000 on the 21st. At 900 mb the dominant nature of the Agnes circulation is quite evident. The Great Lakes relative vorticity maximum is much weaker. The developing rain area across western New York and Pennsylvania at 0000 GMT is embedded in a region of anticyclonic vorticity. At 400 mb the Agnes relative vorticity pattern is considerably weaker with the Great Lakes trough comparable in vorticity strength to the 900 mb value. A separate, weak vorticity maximum center is seen across southern Ohio. This area was centered along the Illinois-Indiana border at 1200 GMT (not shown).

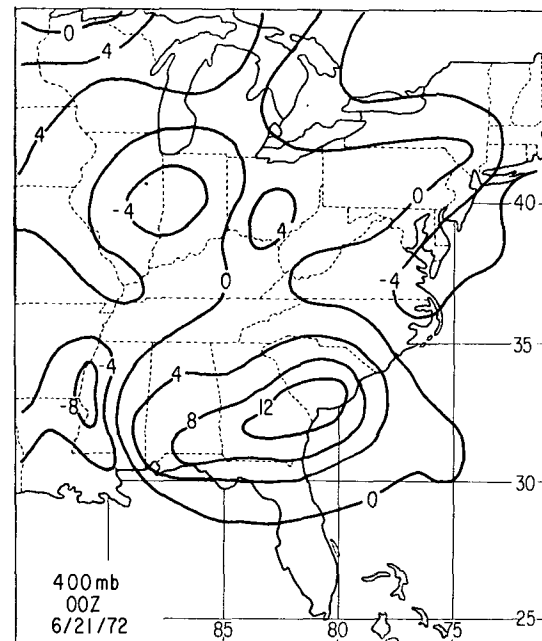
The horizontal moisture flux convergence at 900, 700 and 500 mb is shown in Fig. 9 for the 0000 GMT time period. Strong flux convergence in the vicinity of Agnes and to a lesser extent the Great Lakes frontal trough are connected across the northern Appalachians at 900 mb. The pattern is more confused at 700 mb but moisture flux convergence from Agnes north-northeastward along the Appalachians is suggested with an area of weak moisture flux divergence located immediately to the west and preceding the frontal trough. The moisture flux convergence associated with Agnes at 500 mb is located to the east and south of the surface center with weak flux divergence immediately to the north. A separate zone of moisture flux convergence is seen along the Appalachians from northwestern Georgia into extreme western Pennsylvania.

The sequence of events associated with the heavy rains across western New York and Pennsylvania from 20–21 June 1972 has now been documented. Next we examine the relevant dynamics associated with the development stage of the precipitation region. In addition to horizontal moisture flux convergence, kinematic vertical velocities were computed from the tabulated wind data. Boundary conditions of  $\omega=0$  at 1000 and 150 mb were used along with the O'Brien (1970) quadratic adjustment scheme to the computed horizontal divergences. Resulting values of kinematic vertical velocities from 950 to 250 mb at 100 mb intervals were then computed.

Nonlinear balanced vertical velocities obtained from the State University of New York at Albany (SUNYA) revised version of Krishnamurti's (1968) diagnostic balance model were computed for comparison with the kinematic vertical velocities. Complete details on the revised model format and the diagnostic computations surrounding the conversion of Agnes into an extratropical cyclone can be found in DiMego (1977). A brief summary of the model is given in the Appendix. The 0000 GMT 21 June 1972 period is best suited for a display of the results as that was the



(a)



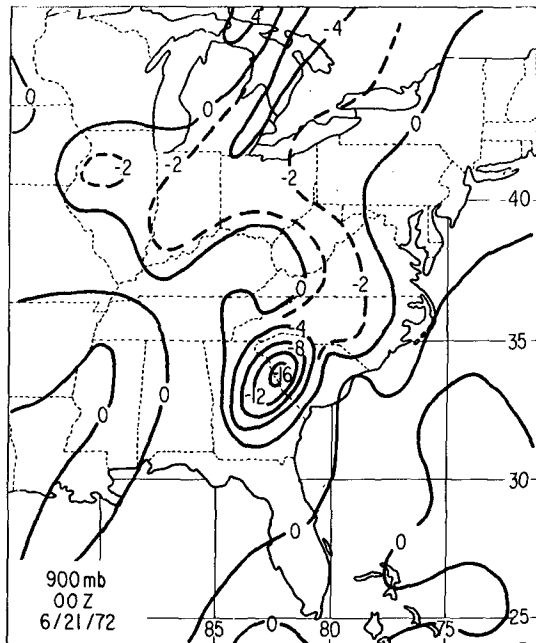
(b)

FIG. 8. 900 mb (a) and 400 mb (b) relative vorticity  $\times 10^{-5} \text{ s}^{-1}$  for 0000 GMT 21 June 1972.

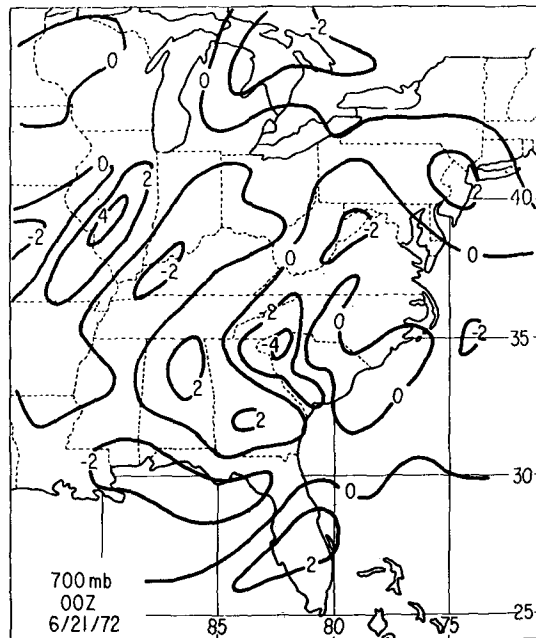
time of rapid development of the precipitation systems.

Fig. 10 shows a vertical cross section along  $40^\circ\text{N}$  of moisture flux convergence and kinematic vertical velocity for the 0000 period. Moisture flux convergence is most pronounced through a substantial tropospheric layer between  $79$  and  $89^\circ\text{W}$ . The magnitude of the

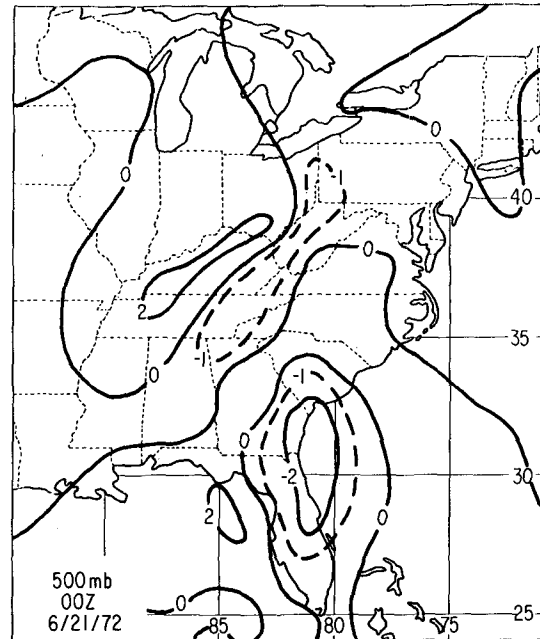
flux convergence increases westward while the vertical extent of the flux convergence weakens. Low-level flux divergence between 80 and 84°W gives way to strong low-level flux convergence around 85–86°W. The outbreak of convective activity across the eastern Great Lakes is then seen to be associated with shallow but strong moisture flux convergence while the western Pennsylvania rain area is embedded in a region of weaker but significantly deeper moisture flux convergence on the synoptic scale.



(a)



(b)



(c)

FIG. 9. 900 mb (a), 700 mb (b) and 400 mb (c) moisture flux convergence  $-\nabla \cdot qV$  ( $10^{-7} \text{ s}^{-1}$ ) for 0000 GMT 21 June 1972.

The kinematic omega cross section shows that the magnitude of the synoptic-scale vertical velocity exceeds  $4 \times 10^{-3} \text{ mb s}^{-1}$  along 85°W with a maximum value of just under  $6 \times 10^{-3} \text{ mb s}^{-1}$  near 600 mb. The maximum magnitude of  $4 \times 10^{-3} \text{ mb s}^{-1}$  along 79°W is located in the vicinity of 450 mb with weak subsidence indicated near the ground. This suggests the possibility that the synoptic-scale physical process responsible for triggering the outbreak of precipitation across western New York and Pennsylvania is concentrated in the mid and upper troposphere.

Figs. 11 and 12 show some of the results of the partitioning of the non-linear balanced omegas at 550 and 350 mb for 0000 GMT 21 June. Included are the contributions due to differential vorticity advection by the nondivergent wind, the Laplacian of thermal advection by the nondivergent wind, the Laplacian of latent heating (stable plus convective), and the total vertical motion field as the sum of the 12 forcing functions listed in the Appendix.

At 550 mb the contribution of thermal advection and differential vorticity advection are of comparable magnitude in the ascent regions. Differential vorticity advection is concentrated northeast of Agnes along the Carolina coast with a separate maximum to the north-northwest in the upper Ohio valley. Two separate ascent centers due to thermal advection are also evident. Latent heat release provides the dominant contribution to upward motion with an area in excess of  $-2.0 \times 10^{-3} \text{ mb s}^{-1}$  north-northeast of Agnes. Note the separate ascent area exceeding  $-1.5 \times 10^{-3} \text{ mb s}^{-1}$

over northwestern Pennsylvania and extreme southwestern New York. Stable heating contributed approximately 60–70% of the total latent heating in this area (DiMego, 1977). According to Buffalo and Pittsburgh WSR-57 radar data, cloud tops were mostly uniform during the rainstorm with no tops exceeding 7300 m.

The picture is rather different at 350 mb. Differential vorticity advection dominates the thermal advection in magnitude and is displaced upstream, especially in the vicinity of Agnes. The upper Ohio Valley center of ascent due to differential vorticity advection is much more pronounced at 350 mb than 550 mb. A weaker ascent area due to the Laplacian of thermal advection is located across extreme southwestern Ontario and eastern Lake Erie in advance of the center due to differential vorticity advection. The latent heat contribution to ascent is considerably weakened at 350 mb with the maximum concentration to the south and east of Agnes. A very weak ascent area is still evident, however, across western Pennsylvania.

Finally, the resulting total omega fields reflect primarily the contribution of these three forcing functions. The two separate ascent centers seen at 550 mb merge into one center with a north-northwestward extension at 350 mb. The highly asymmetric nature of the vertical motion patterns with respect to Agnes is in reasonable agreement with the rainfall results presented earlier.

## 7. Summary

In summary, the diagnostic results suggest that differential vorticity advection in the mid and upper troposphere associated with a weak short wave at the southern edge of the Great Lakes trough provided the initial triggering mechanism for the growth of the ascent area across the Ohio Valley, separate from the Agnes circulation to the south. Evidence for this short wave is also given by the observed wind, height and temperature data (Fig. 7) and resulting relative vorticity field (Fig. 8). Thermal advection is most significant at 550 mb with the region of strongest ascent displaced downstream from that due to differential vorticity advection. Latent heat release plays a dominant role in the resulting total omega field downstream of the region of maximum differential vorticity advection.

Surface development in response to the Great Lakes short wave was twofold. First, an area of light rain developed in the Ohio Valley around 1200 on the 20th. This rain area advected slowly northeastward while slowly intensifying. It reached into western Pennsylvania and southwestern New York by 0000 on the 21st. The heaviest rain fell in the Chemung valley area of New York around Wellsville in the 17 h ending 1400 GMT 21 June. The observed surface data suggest that this rain was mostly stable in origin (recall also

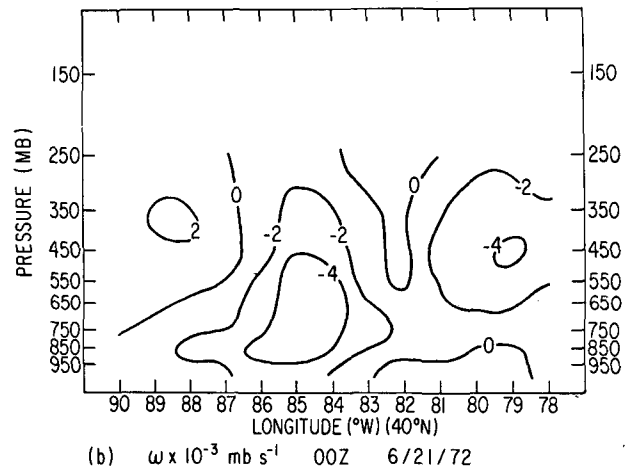
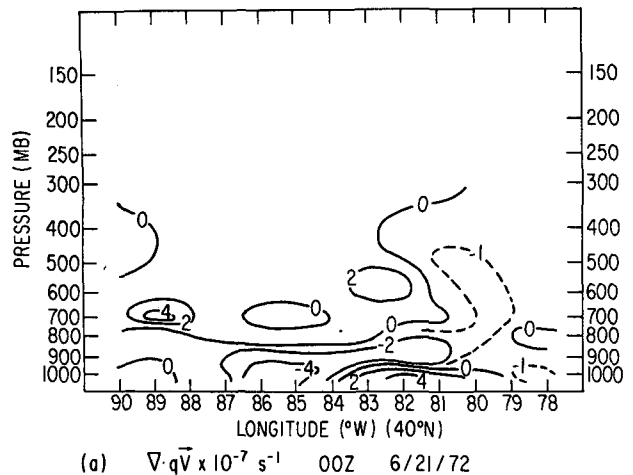


FIG. 10a. Vertical cross section along 40°N of moisture flux convergence  $-\nabla \cdot q\bar{V} (10^{-7} \text{ s}^{-1})$  for 0000 GMT 21 June 1972.

FIG. 10b. As in Fig. 10a except for kinematic omega  $\times 10^{-3} \text{ mb s}^{-1}$ .

Fig. 2). No thunderstorms were reported embedded in the rain area from the surface network or radar observations. The resulting flooding in the Chemung valley was produced by rains of 2–3 cm h<sup>-1</sup> which lasted approximately 12 h.

The second significant surface development was the existence of a squall line which originated across eastern Michigan and extreme northwestern Ohio shortly before 1800 GMT 20 June and moved east-northeastward before dissipating near 0600 GMT 21 June. The potential for convection in this area is seen from a tongue of low lifted index across this area at 0000 on the 21st (Fig. 3). Between these two systems no significant rains are observed. Some understanding for this observation is seen in the surface and lower and mid-troposphere moisture flux convergence patterns of Figs. 5 and 9 at this time. Moisture flux divergence is present between the squall line area and western Pennsylvania rain areas at the surface and 700 mb. Weak moisture flux convergence

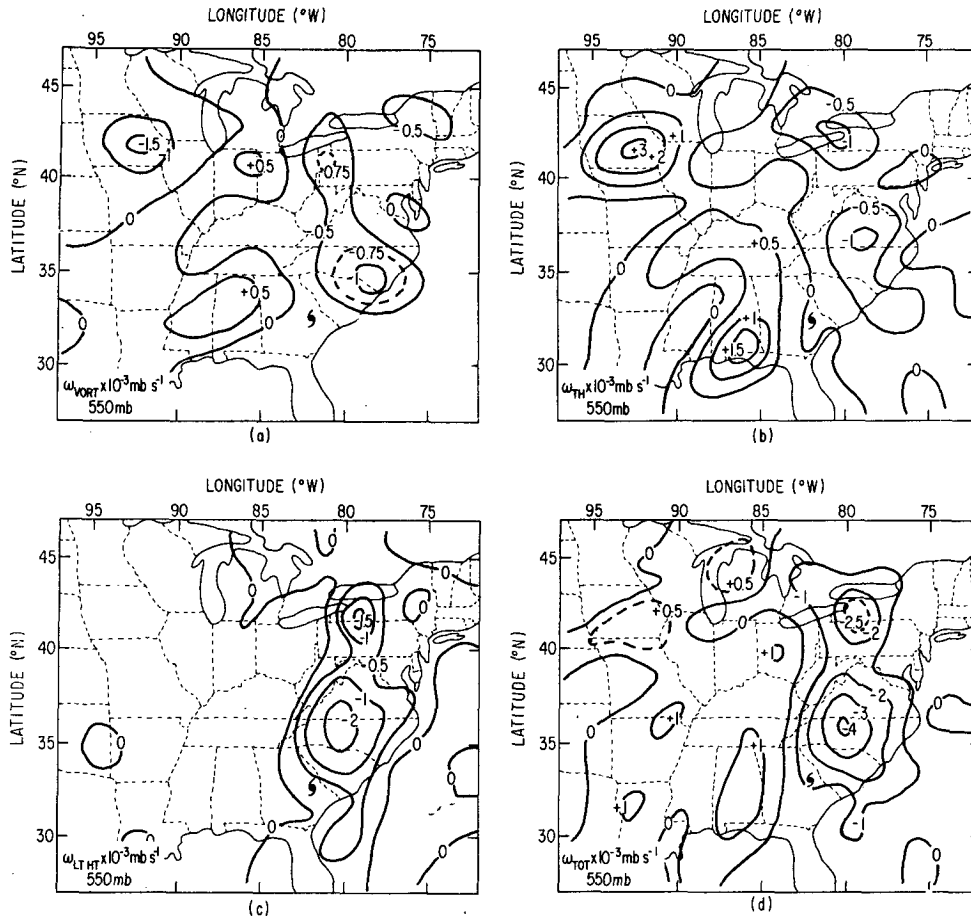


FIG. 11a. Nonlinear balanced contribution to vertical motion from differential velocity advection by the nondivergent wind  $\times 10^{-3} \text{ mb s}^{-1}$  for 550 mb at 0000 GMT 21 June 1972.

FIG. 11b. As in Fig. 11a except for the Laplacian of thermal advection by the nondivergent part of the wind.

FIG. 11c. As in Fig. 11a except for the Laplacian of latent heating.

FIG. 11d. As in Fig. 11a except for the total nonlinear balanced omega.

extends across the entire region at 900 mb although there is a definite concentration of moisture flux convergence near Agnes and northward along the Appalachians as well as a narrow, well-defined tongue across eastern Michigan and Lake Huron. Moisture flux convergence into western Pennsylvania extends north-northeastward from Agnes as well as from the Atlantic at 700 mb. At 500 mb moisture flux convergence extends from the eastern periphery of the Agnes circulation northwestward toward the Appalachians.

The apparent conclusion would be that the initial Ohio Valley rain area was made more potent and long lasting by moisture flux convergence north of Agnes along the Appalachians in the lower troposphere superimposed below moisture flux convergence from the Atlantic in the mid-troposphere. Latent heat release, once triggered, was then the dominant factor in contributing to the total upward motion pattern across western Pennsylvania and New York. The

complete moisture budget for this case and related important questions on computed versus observed rainfall along with an assessment of the moisture available for convection are a part of a companion paper (Carr and Bosart, 1978).

## 8. Conclusions

A lesson from the Wellsville flood disaster is that an intrusion of tropical moisture into a relatively mountainous area in advance of a slow moving upper disturbance creates a *potential* for flooding given the proper meteorological, geographical and hydrological factors.

The observed data and resulting diagnostic computations then suggest the schematic picture shown in Fig. 13 which may have some general validity. Strong consideration must be given to the potential for flooding in the confluent region shown by the hatched area (region A) well in advance of the possible



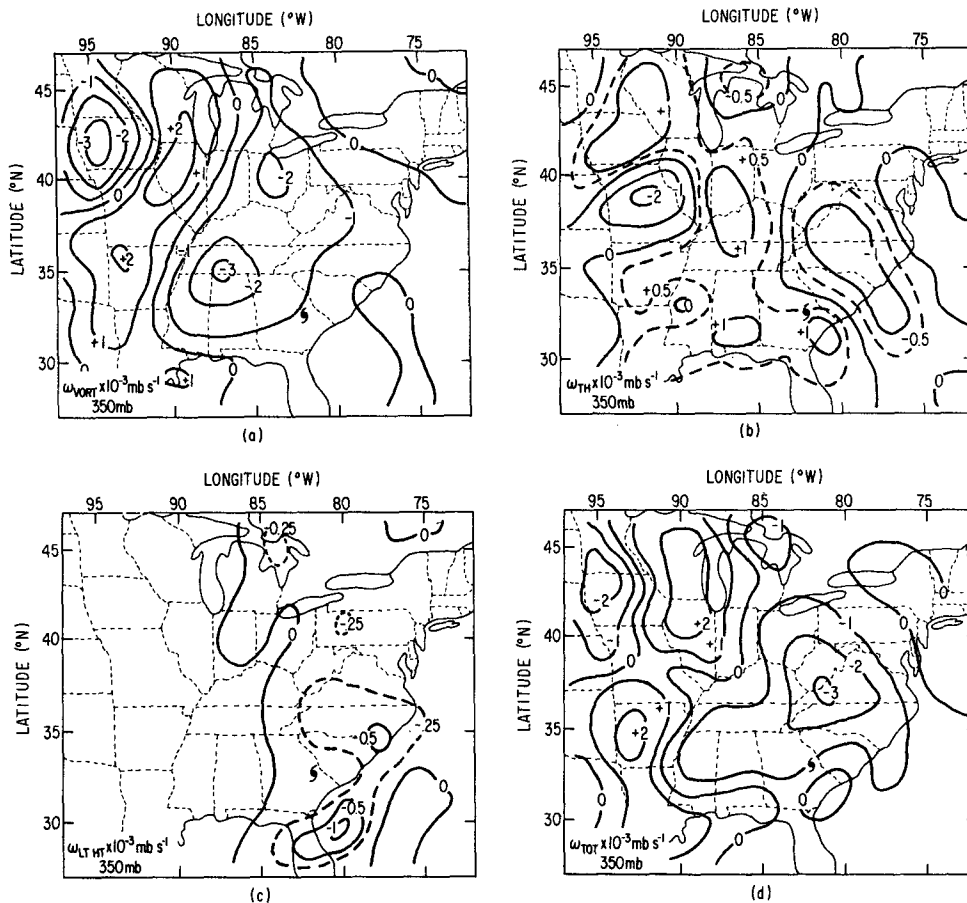


FIG. 12. As in Fig. 11 except for 350 mb.

advent of heavy rains associated with the tropical system to the south (region B). This flooding potential will be enhanced for very slow moving systems because of the persistent strong and deep tropospheric moisture convergence pattern to the east of the tropical system. The approach of a mid and upper tropospheric short wave trough toward the confluent region in the northern branch of the westerlies, even if apparently quite weak, must be viewed as a possible triggering mechanism. In addition, these short wave troughs have a tendency to be much better defined by the observed winds as opposed to the height field and as a consequence may be diminished in intensity or smoothed out by conventional objective analysis schemes.

Appalachian rains associated with tropical storm Eloise in September 1975 illustrate some similarities as well as significant differences to the Agnes situation. While the resulting surface rainfall distribution across Pennsylvania was similar for Agnes and Eloise as Schlegel (1976) points out, the physical mechanism was apparently quite different. Although we have not made any detailed diagnostic computations for Eloise, a careful inspection of the surface and upper air maps for this case suggests that thermal advection played

a much more dominant role in the resulting lower and mid-tropospheric vertical velocity pattern.

Eloise interacted with a major baroclinic trough at

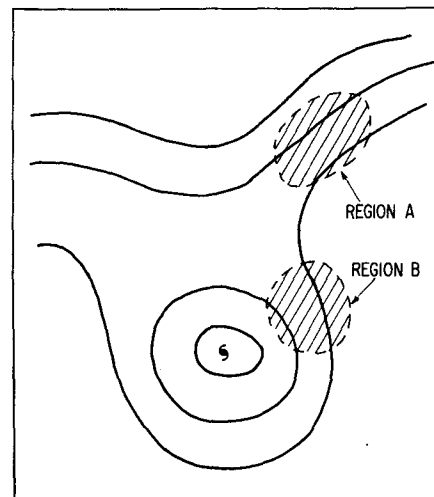


FIG. 13. Schematic of mid-tropospheric stream lines associated with possible tropical storm related flooding.

low latitudes across the United States. A split flow pattern prevailed with another branch of the westerlies across the northern United States and southern Canada. Substantial baroclinicity was then maintained across most of the central and northern United States such that the development of a strong surface anticyclone across New England in the wake of one short wave set the stage for persistent lower tropospheric easterly flow and warm advection in the central and northern Appalachian region. Agnes, on the other hand, was associated with little baroclinicity in the vicinity of the circulation itself until the extratropical phase began late in the day on 22 June 1972.

*Acknowledgments.* We would like to thank Professor T. N. Krishnamurti for providing us with the original version of his nonlinear balanced omega model. Geoffrey J. DiMego rendered assistance in the diagnostic computations. Debra Fondario, Benjamin Novograd and David Palmiero provided assistance in the data plotting. The manuscript was typed by Sally Young. The research was supported by National Science Foundation under Grant A023897-002.

#### APPENDIX

##### Nonlinear Balance Model

The nonlinear balanced omega model used for the diagnostic computations was originally presented by Krishnamurti (1968). The modified version as used at SUNYA is described by DiMego (1977). The governing equations are as follows:

##### Vorticity equation

$$\frac{\partial}{\partial t} \nabla^2 \psi = -J(\psi, \nabla^2 \psi) - \beta \frac{\partial \psi}{\partial x} - g \frac{\partial}{\partial p} \left( \frac{\partial \tau_y}{\partial x} - \frac{\partial \tau_x}{\partial y} \right) + \nabla \chi \cdot \nabla \zeta_a$$

$$+ \zeta_a \nabla^2 \chi - \nabla \omega \cdot \nabla \frac{\partial \psi}{\partial p} - \omega \frac{\partial}{\partial p} \nabla^2 \psi.$$

##### Omega equation

$$\nabla^2 \sigma \omega + f^2 \frac{\partial^2 \omega}{\partial p^2} = f \frac{\partial}{\partial p} J(\psi, \zeta_a) + \pi \nabla^2 J(\psi, \theta)$$

$$- 2 \frac{\partial}{\partial t} \frac{\partial}{\partial p} J \left( \frac{\partial \psi}{\partial x}, \frac{\partial \psi}{\partial y} \right) - f \frac{\partial}{\partial p} (\zeta \nabla^2 \chi)$$

$$+ f \frac{\partial}{\partial p} g \frac{\partial}{\partial p} \left( \frac{\partial \tau_y}{\partial x} - \frac{\partial \tau_x}{\partial y} \right) - \frac{R}{c_p p} \nabla^2 H_L$$

$$- \frac{R}{c_p p} \nabla^2 H_S + f \frac{\partial}{\partial p} \left( \omega \frac{\partial}{\partial p} \nabla^2 \psi \right)$$

$$+ f \frac{\partial}{\partial p} \left( \nabla \omega \cdot \nabla \frac{\partial \psi}{\partial p} \right) - f \frac{\partial}{\partial p} (\nabla \chi \cdot \nabla \zeta_a)$$

$$- \pi \nabla^2 (\nabla \chi \cdot \nabla \theta) - \beta \frac{\partial}{\partial p} \frac{\partial \psi}{\partial y} \frac{\partial \psi}{\partial t}$$

##### Continuity equation

$$\nabla^2 \chi = \frac{\partial \omega}{\partial p}$$

The grid distances are  $\Delta x = 1^\circ$  longitude,  $\Delta y = 1^\circ$  latitude,  $\Delta p = 100$  mb with  $\omega$  defined on the 950, 850, 750, 650, 550, 450, 350, 250 and 150 mb surfaces.  $\partial \psi / \partial t$  and  $\chi$  appear every 100 mb from 1000 to 100 mb. All other computational details are found in DiMego (1977).

The relevant symbols are defined as follows:

$f$	Coriolis parameter
$\omega$	vertical velocity [ $= dp/dt$ ]
$J$	Jacobian operator
$\psi$	rotational part of the horizontal wind
$\chi$	velocity potential
$\zeta_a$	absolute vorticity
$\beta$	northward variation of Coriolis parameter
$\theta$	potential temperature
$\tau_x, \tau_y$	frictional stress
$H_L$	latent heat flux
$H_S$	sensible heat flux

#### REFERENCES

- Carr, F. H., and L. F. Bosart, 1978: A diagnostic evaluation of rainfall predictability for Tropical Storm Agnes, June 1972. *Mon. Wea. Rev.*, **106**, 348-359.
- DeAngelis, R. M., and W. T. Hodge, 1972: Preliminary Climatic Data Report Hurricane Agnes June 14-23, 1972. NOAA Tech. Memo. EDS NCC-1, National Climatic Center, Asheville, N.C., 62 pp.
- DiMego, G. J., 1977: A diagnostic study of the transformation of Tropical Storm Agnes into an extratropical cyclone. Ph.D. dissertation, State University of New York at Albany, 277 pp.
- Krishnamurti, T. N., 1968: A diagnostic balance model for studies of weather systems of low and high latitudes, Rossby number less than 1. *Mon. Wea. Rev.*, **96**, 197-207.
- O'Brien, J. J., 1970: Alternative solutions to the classical vertical velocity problem. *J. Appl. Meteor.*, **9**, 197-203.
- Schlegel, J., 1976: A comparison of Hurricane Eloise and Hurricane Agnes. *Weatherwise*, **29**, 70-73.